

A first-principles study on zigzag phosphorene nanoribbons terminated by transition metal atoms

Shuai Yang(杨帅), Zhiyong Wang(王志勇)†, Xueqiong Dai(戴学琼), Jianrong Xiao(肖剑荣), and Mengqiu Long(龙孟秋)

Citation: Chin. Phys. B, 2021, 30 (**2**): 027305. DOI: 10.1088/1674-1056/abc0e1
Journal homepage: http://cpb.iphy.ac.cn; http://iopscience.iop.org/cpb

What follows is a list of articles you may be interested in

General principles to high-throughput constructing two-dimensional carbon allotropes

Qing Xie(谢庆), Lei Wang(王磊), Jiangxu Li(李江旭), Ronghan Li(李荣汉), Xing-Qiu Chen(陈星秋)
Chin. Phys. B, 2020, 29 (**3**): 037306. DOI: 10.1088/1674-1056/ab6c4b

Defect engineering on the electronic and transport properties of one-dimensional armchair phosphorene nanoribbons

Huakai Xu(许华慨), Gang Ouyang(欧阳钢)
Chin. Phys. B, 2020, 29 (**3**): 037302. DOI: 10.1088/1674-1056/ab69ec

Black phosphorus-based field effect transistor devices for Ag ions detection

Hui-De Wang(王慧德), David K Sang, Zhi-Nan Guo(郭志男), Rui Cao(曹睿), Jin-Lai Zhao(赵劲来), Muhammad Najeeb Ullah Shah, Tao-Jian Fan(范涛健), Dian-Yuan Fan(范滇元), Han Zhang(张晗)
Chin. Phys. B, 2018, 27 (**8**): 087308. DOI: 10.1088/1674-1056/27/8/087308

Double band-inversions of bilayer phosphorene under strain and their effects on optical absorption

Shi He(何诗), Mou Yang(杨谋), Rui-Qiang Wang(王瑞强)
Chin. Phys. B, 2018, 27 (**4**): 047303. DOI: 10.1088/1674-1056/27/4/047303

Van der Waals heterostructure of phosphorene and hexagonal boron nitride: First-principles modeling

Peng Zhang(张鹏), Jing Wang(王静), Xiang-Mei Duan(段香梅)
Chin. Phys. B, 2016, 25 (**3**): 037302. DOI: 10.1088/1674-1056/25/3/037302

A first-principles study on zigzag phosphorene nanoribbons terminated by transition metal atoms*

Shuai Yang(杨帅)[1], Zhiyong Wang(王志勇)[1,†], Xueqiong Dai(戴学琼)[2], Jianrong Xiao(肖剑荣)[1], and Mengqiu Long(龙孟秋)[3]

[1] College of Science, Guilin University of Technology, Guilin 541008, China
[2] Modern Education Technology Center, Guilin University of Technology, Guilin 541008, China
[3] Hunan Key Laboratory of Super Micro-structure and Ultrafast Process, Central South University, Changsha 410083, China

(Received 14 July 2020; revised manuscript received 30 September 2020; accepted manuscript online 14 October 2020)

We have investigated the electronic and magnetic properties of zigzag phosphorene nanoribbons (ZPNRs) with transition metal (TM) passivated atoms, it can be found that the ZPNRs with TM passivated atoms exhibit different magnetisms except for the Ni-passivated system. Meanwhile, the results show that the magnetic moments of ZPNRs with TM passivated atoms are larger than that of ZPNRs with other passivated non-metals/groups. Interestingly, it can be found that Fe-passivated ZPNR exhibits magnetic semiconducting character, which provides the possbility for the application of phosphorene in information storage. For Mn-passivated ZPNRs, it exhibits the half-metallicity. These results may be useful for potential applications of phosphorene in electronic and high-performance spintronic devices.

Keywords: phosphorene, first-principles calculations, half-metallicity, passivated

PACS: 73.22.–f, 75.75.–c, 74.20.Pq **DOI:** 10.1088/1674-1056/abc0e1

1. Introduction

After the discovery of graphene,[1] others new two-dimensional nanomaterials have attracted much attention of researchers, such as silicene,[2] transition metal dichalcogenides,[3] and so on. In recent years, phosphorene has been realized from bulk materials by mechanical exfoliation method.[4–8] This new two-dimensional[9] material has attracted enough attention in academic communities. Compared to zero-band gap graphene,[1] the great advantage of phosphorene is its adjustable band gap, which allows the phosphorene to be applied from visible to infrared regions of the spectrum.[10] Meanwhile, it is a semiconductor with direct band gap,[9] which strongly depends on the number of layers,[10,11] ranging from 0.59 eV (five-layer)[12] to 2.0 eV (monolayer).[8] In contrast to the MoS_2 with low carrier mobility,[13] phosphorene-based field effect transistors (FETs) have very high charge carrier mobility up to 1000 $cm^2/(V{\cdot}s)$ at room temperature, and high on/off ratio up to 10^4. In addition, it exhibits ambipolar performance with drain current modulation on the order of 10^5.[5,10,12,14–16] Due to the unique buckled honeycomb structure,[17] phosphorene also has potential applications in thermoelectric materials.[18,19]

Similar to graphene nanoribbons (GNRs), they have different edge geometries, namely, zigzag phosphorene nanoribbons (ZPNRs) and armchair phosphorene nanoribbons (APNRs), their electronic properties are dependent on edge structures of the ribbons. Guo *et al*. reported that the pristine ZPNRs are metal, while the pristine APNRs are semiconductor with indirect bandgaps.[20,21] For one-dimension (1D) nanoribbons, edge engineering and introducing defects have been considered to be the crucial way to tune various properties of materials.[22,23] For APNRs, it is found that it is a direct or indirect bandgap semiconductor, and the band gap depends on the edge functionalization groups.[24] For Mn-passivated edge, it exhibits half-semiconductor electrical properties in the ferromagnetic state.[25] Due to the stronger quantum size effect and edge state of ZPNRs,[26–28] different edge passivations have a significant influence on its electronic properties. The hydrogenated ZPNRs exhibit a direct band gap nonmagnetic semiconducting behaviors, while the O-passivated ZPNRs show magnetic ground states.[21,29] The electronic structure and magnetic properties of ZPNRs terminated with different edge-functionalizations have been systematically studied, and the results showed that the ZPNRs exhibit half-metal phase.[30] Due to the d orbital of transition metals being more delocalized than the p orbital of non-metals,[31] the magnetic properties of Fe-passivated ZPNRs with different widths are investigated, it is found that the Fe-passivated ZPNRs show different properties from ZPNRs with passivated non-metal atoms/groups.[32] However, a systematic study of ZPNRs with transition metal (TM) passivated atoms is still absent.

In this paper, we theoretically study the effect of TM

*Project supported by the National Natural Science Foundation of China (Grant No. 11564008), the Natural Science Foundation of Guangxi Zhuang Autonomous Region, China (Grant No. 2017GXNSFAA198195), and the Shanghai Supercomputer Center.

†Corresponding author. E-mail: zhiyongwang@glut.edu.cn

© 2021 Chinese Physical Society and IOP Publishing Ltd

(Sc-Ni) atoms passivation on electronic structures and magnetic properties of ZPNRs. The results show that the magnetic moments of ZPNRs with TM passivated atoms are larger than those of ZPNRs with other passivated non-metals/groups. Meanwhile, the calculated results also show that Mn-ZPNRs exhibit half-metallicity state, which provides the possiblity for designing high-performance spintronic devices.

2. Calculation methods

We have performed the first-principles based on density functional theory (DFT) by using Spanish Initiative for Electronic Simulations with Thousands of Atoms (SIESTA)[33–36] package. The generalized gradient approximation (GGA) with Perdew–Burke–Ernzerhof (PBE)[37,38] functional is used to describe the exchange–correlation functional. The atomic orbital basis set is a double-ζ plus polarization function (DZP). The optimized lattice constants of the unit cell are 4.623 Å and 3.298 Å, respectively. Taking the calculation efficiency and accuracy into consideration, a mesh cutoff of 200 Ry (1 Ry = 13.6056923 eV) and a $1\times11\times1$ Monkhorst–Pack k-point grid are applied. And Mulliken charge analysis is used to calculate the charge transfer between the TM atoms and the phosphorene.

In order to assess the stability of the phosphorene system with TM-passivated atoms, the binding energy (E_b) is defined as

$$E_b = (E_{TM-ZPNRs} - E_{ZPNRs} - 8E_{TM})/8,$$

where $E_{TM-ZPNRs}$ and E_{ZPNRs} stand for the total energy of ZPNRs with and without TM-passivated atoms, respectively.[32] E_{TM} is the energy of single transition atom in vacuum, E_b can reflect the stability of ZPNRs with TM-passivated atoms, and a more negative value corresponds to a more stable edge passivation.

3. Results and discussion

In the present study, we have investigated the magnetic and electronic properties of ZPNRs with eight TM-passivated atoms (Sc, Ti, V, Cr, Mn, Fe, Co, and Ni). For the case of passivation modulation, we have made descriptions of the method and calculation in detail. The results are shown in Fig. 1. In order to determine the bonding between TM atoms and P atoms, the E_b of the ZPNRs with different passivated atoms are calculated. As shown in Table 1, E_b corresponds to the case when the width of ZPNR is $N = 8$. It is not difficult to find that the binding energy of all TM-passivated atoms phosphorene nanoribbons are negative (Fig. 2(a)), which reflects the stability of ZPNRs with TM-passivated atoms, and a more negative value corresponds to a more stable edge passivation.[32]

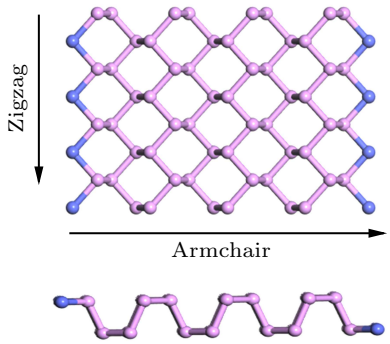


Fig. 1. Top and side views of ZPNRs, the nanoribbon edge is along the zigzag direction, the nanoribbon width is along the armchair direction. The P atoms and TM atoms are shown in purple and blue, respectively.

Magnetic behavior is an important aspect of phosphorene with TM-passivated atoms. Therefore, the magnetic moments of ZPNRs with different TM-atom edge passivations are also calculated. The calculated results are shown in Table 1, the magnetic moments of TM atoms and TM-ZPNRs are in accordance as shown in Fig. 2(b). It is interesting to see that all TM-ZPNRs exhibit magnetic properties except for Ni-ZPNR configuration, which magnetic moment is always zero and behaves no magnetism. Among all TM-ZPNRs magnetic configurations, the Mn-ZPNR is particularly special, its magnetic moment decreases by only 0.01 μ_B compared to the free Mn atom (as shown in Table 1). According to the charge transfer shown in Fig. 2(c), it can be clearly observed that the charge transfer amount of Mn-ZPNR is up to 0.283 e among the TM-ZPNRs configurations. It may be attributed to that the Mn atom interacts strongly with the surrounding phosphorus atoms, and the surrounding phosphorus atoms have stronger electronegative charge transfer as the charge acceptor. In contrast, the magnetic moments of ZPNRs with passivated Sc, Ti, Cr, Mn, Fe, and Co have decreased by 0.68, 1, 0.68,1.55, 0.51, and 0.83 μ_B in comparison with the magnetic moment of the free TM atoms, respectively. In order to explore the mechanism of the induced magnetic moment, the Mulliken charge analysis and the migration rate between 4s and 3d orbitals of various TM atoms are calculated and listed in Table 1. The electronic state of the initial 4s orbital and 3d orbital can be clearly observed from Table 1, it is seen that the charge transfer appears between TM atoms and P atoms. In Ni-ZPNRs system, it can be found that the 4s orbital donates 1.12 electrons and transfers 0.42 electrons to 3d orbital. In addition, it is worth noting that 0.7 electrons have migrated to the 4p orbital, which may be the reason that the magnetic moment of Ni-ZPNR is 0. As shown in Fig. 2(c), the Ni atom gets electrons from the surrounding phosphorus atoms. The calculated results are in accordance with the previous results.[32] For the case of V-ZPNRs system, it can be seen that the 4s orbital donates 1.3 electrons and transfers 0.52 electrons to 3d orbital, and transfers 0.674 electrons to 4p orbital. The reduced magnetic moment may be attributed to the reduced unpaired

Table 1. Edge structure parameter of optimized TM-ZPNRs with $N = 8$. $d_{\mathrm{TM-P}}$, $d^1_{\mathrm{p-p}}$, and $d^2_{\mathrm{p-p}}$ refer to the lengths (in unit Å) of TM–P bonds and P–P bonds in the vertical and horizontal directions, respectively. E_{b} stands for the binding energy (in unit eV). μ and μ_0 (in unit μ_{B}) correspond to the magnetic moments of TM-ZPNRs and free TM atoms, respectively. 4s/3d (e) refer to the valence electron configurations for a free-standing TM atom. 4s*/3d*/4p* (e) is the valence electron configurations corresponding to the TM atom's Mulliken charge analysis of the TM-ZPNRs.

	$d_{\mathrm{TM-P}}$	$d^1_{\mathrm{p-p}}$	$d^2_{\mathrm{p-p}}$	E_{b}	μ/μ_0	4s/3d	4s*/3d*/4p*
ZPNRs	–	2.26	2.22	–	–	–	–
Sc-8	2.595	2.222	2.329	–3.61	1.32/2	2/1	0.724/1.5/0.734
Ti-8	2.478	2.235	2.301	–2.60	2.00/3	2/2	0.742/2.484/0.74
V-8	2.476	2.238	2.297	–3.37	3.32/4	2/3	0.702/3.52/0.674
Cr-8	2.465	2.259	2.306	–2.52	4.45/6	1/5	0.72/4.617/0.648
Mn-8	2.429	2.265	2.294	–4.48	4.99/5	2/5	0.848/5.074/0.795
Fe-8	2.309	2.419	2.266	–3.40	3.49/4	2/6	0.871/6.17/0.791
Co-8	2.244	2.308	2.398	–3.32	2.17/3	2/7	0.785/7.252/0.824
Ni-8	2.178	2.315	2.344	–3.64	0/2	2/8	0.877/8.419/0.743

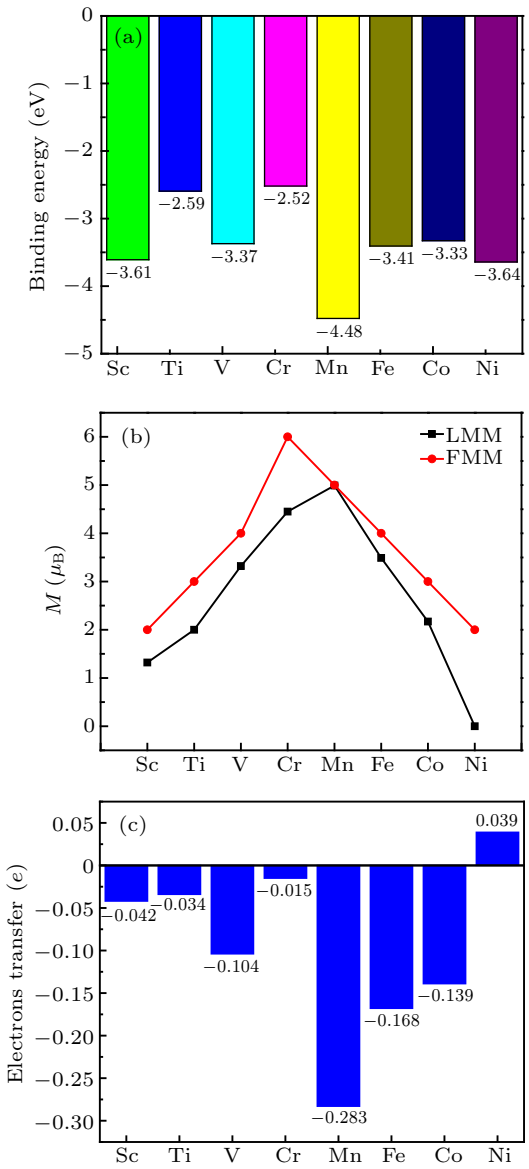


Fig. 2. (a) Binding energy of the TM-ZPNRs. (b) The magnetic moment μ (in unit μ_{B}) refers to the local magnetic moment (LMM) of the TM atoms in the TM-ZPNRs, and μ_0 (in unit μ_{B}) refers to the magnetic moment of the free (FMM) TM atoms, corresponding to the black line and the red line, respectively. (c) Electrons transfer between the TM atoms and the ZPNRs.

electrons because of the charge transfer between ZPNRs and TM atoms. The magnetic moment of the V-ZPNRs system is reduced from 4 μ_{B} to 3.32 μ_{B}. For the Fe-ZPNRs configuration, it can be found that 0.17 electrons are transferred from 4s orbital to 3d orbital, reducing the unpaired electrons of 3d orbital and resulting in the decrease of magnetic moment from 4 μ_{B} (free standing state) to 3.49 μ_{B}. The remaining configurations are similar to the case of Fe-ZPNRs. Based on the Mulliken charge analysis, the reduction of magnetic moments may be ascribed to 4s–3d electron transfer and the decrease of unpaired electrons. In addition, the electron transfer between the 4p orbital and the 3d orbital makes the 3d orbital half-filled, which may also cause the reduced magnetic moment of TM-ZPNRs.

After structural relaxation, all structures have greatly distorted compared to the perfect phosphorene nanoribbons, and their distorted degrees depend on the type of 3d atoms, the possible reason is that the 3d atoms have larger atomic radii. We have compared the cases of TM-ZPNRs ($N = 8$) with other calculation results (Table 1), and found that the bond lengths do not change significantly with the increase of the ribbon width.

In order to further understand the change of magnetic moment, the partial density of states (PDOS) of TM-ZPNRs is calculated and shown in Fig. 3. It can be observed that the PDOS of the TM-ZPNRs has changed significantly in the vicinity of the highest valence band and the lowest conduction band as shown in Fig. 3. Here, for the sake of analysis, we divide all the TM-ZPNRs into four types. Among them, Sc, V, Cr, Co passivated ZPNRs are of the same type. In Figs. 3(a), 3(c), 3(d), and 3(g), it can be found that the spin splitting of the TM atoms and the P atoms near the Fermi level is much stronger. By observing the valence electron configurations of Table 1, it can be attributed to the electron transfer from the 4s orbital to the 3d orbital and the 4p orbital. Meanwhile, it can be found that the 3d orbit–spin splitting of TM atoms has wave-function overlap with the 3p orbital of the P atom, which leads to their considerable interactive coupling. In comparison with the bare phosphorene, it is revealed that the magnetism is mainly induced by the electron spin splitting in the 3d orbital of the TM atoms. Actually, the pristine phosphorene exhibits metallic character but no magnetic properties. The terminated Sc (V, Cr, Co) atoms can introduce magnetic properties while

maintain the metallic character of ZPNRs, which may be useful for the design and application of phosphorene-based spintronic devices.

Here, we take the ZPNRs with passivated Ti atom and Fe atom systems as the same type. The total density of states (TDOS) of the ZPNRs with Ti passivated atom and Fe passivated atom is calculated and shown in Figs. 3(b) and 3(f), respectively. It is found that the transiton appears from metal to magnetic semiconductor for the ZPNRs with Ti-passivated atom and Fe-passivated atom. Meanwhile, there are some differences between Ti-ZPNR and Fe-ZPNR. For Ti-passivated ZPNRs, the Ti atoms play a dominant role in the conduction band minimum (CBM) and the valence band maximum (VBM) near the Fermi level (as shown in spin-up PDOS of Fig. 3(b)), and the band gap is approximately 0.24 eV. In contrast, for the spin-down PDOS it is found that that the P atoms play a dominant role near the Fermi level. For Fe-passivated ZPNRs, the P atoms dominate the CBM and VBM according to the spin-up PDOS. The band gap is approximately 0.16 eV.

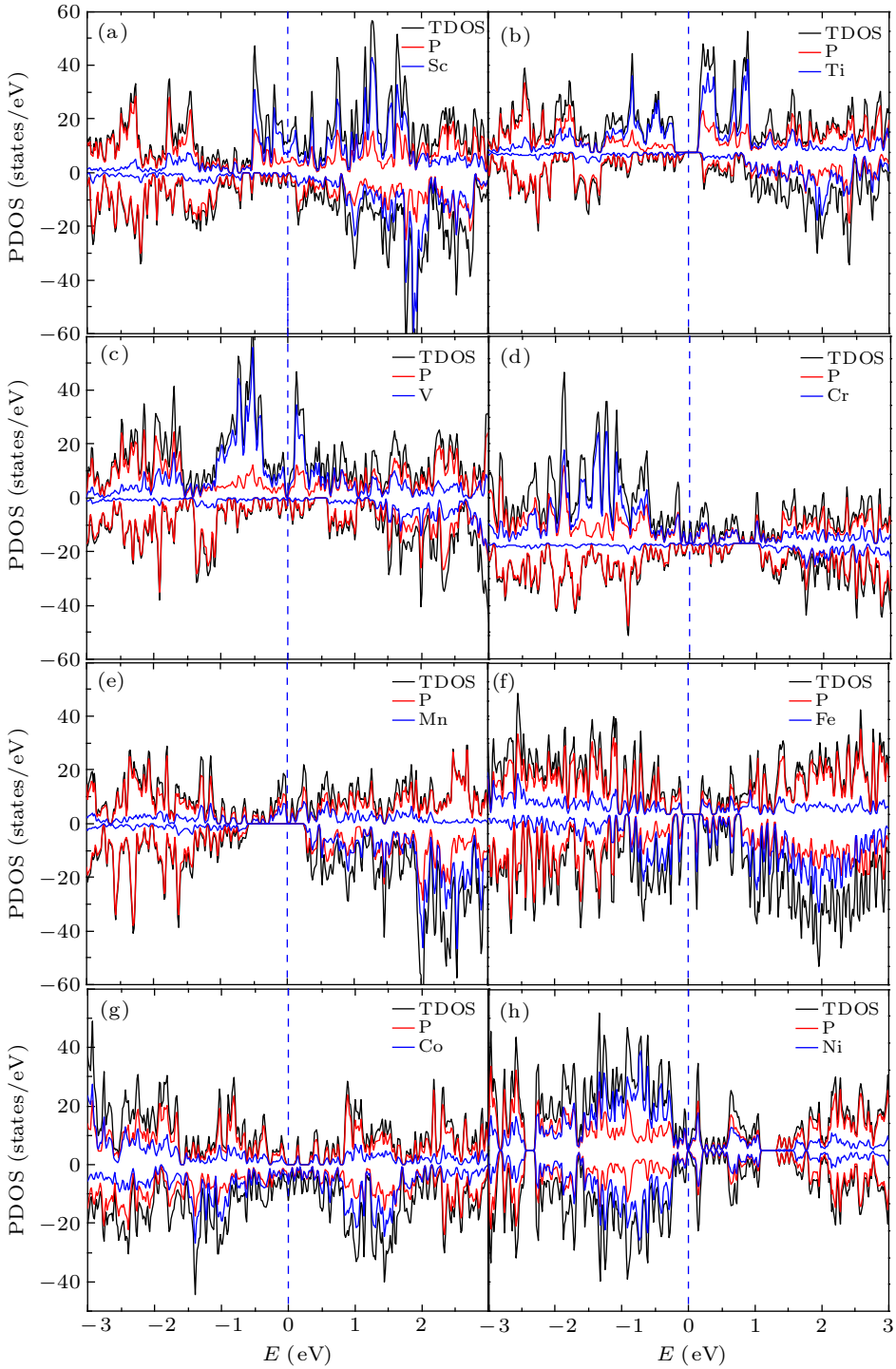


Fig. 3. The projected density of states of ZNPRs with TM (Sc, Ti, V, Cr, Mn, Fe, Co, and Ni)-passivated atoms. The Fermi energy is shifted to zero as indicated by the vertical dotted blue line.

In contrast, for the spin-down PDOS it is found that the Fe atoms paly a dominant role near the Fermi level. The band gap is approximately 0.05 eV. This indicates that the ZPNRs with TM-passivated atoms can modulate the band gap, it is in occordance with the previous work.[39]

For the Mn-ZPNR configuration, it is found that the band gap of the spin-up state is closed and that of spin-down state is still open, namely, the Mn-ZPNR configuration exhibits the half-metallic character. According to Figs. 2(a) and 2(c), it is found that Mn-ZPNR has the largest binding energy and the largest charge transfer. This indicates that Mn-ZPNR may be useful for the application in magnetic storage. However, the interesting results for Ni-passivated ZPNRs appear: the Ni atom is a charge acceptor during the process of charge transfer, and the Ni-ZPNR configuration shows no magnetism and still behaves as a metal, it is similar to pristine ZPNRs.[21] The main reason may be that the Fermi level shifts down due to the presence of Ni atoms, which is in accordance with Table 1 and Fig. 2(c). From the results investigated in this paper, it is hoped that our calculated results may be useful in applications for spintronics and optoelectronics.

4. Conclusions

In summary, we have performed DFT calculations in order to investigate the electronic and magnetic properties of TM-ZPNRs with $N = 8$, and it is demonstrated that the magnetic behavior of ZPNRs can be effectively modulated by the edge passivation of the TM atoms. Because of the different electronegativities between TM and P atoms, the ionic covalent bond is produced, which may be the cause of magnetic properties. In addition, due to the charge transfer, the magnetic moment caused by the d orbital of the TM atom is nonfull occupied, which may be another reason. The Co and Fe terminated ZPNRs exhibit metal and magnetic semiconductor, respectively. While the Mn-ZPNR appears the half-metallic character. These fascinating properties of TM-ZPNRs show that they have great potential applications in future high-performance spintronic devices, optoelectronic devices, and information storage.

References

[1] Novoselov K S, Geim A K, Morozov S V, Jiang D, Zhang Y, Dubonos S V, Grigorieva I V and Firsov A A 2004 *Science* **306** 666

[2] Zhang D, Long M Q, Cui L L, Xiao J and Pan C N 2018 *Organic Electronics* **62** 253

[3] Dong Y L, Zeng B W, Xiao J, Zhang X J, Li D D, Li M J and Long M Q 2018 *J. Phys.: Condens. Matter* **30** 125302

[4] Fei R X, Faghaninia A, Soklaski R, Yan J A, Lo C and Yang L 2014 *Nano Lett.* **14** 6393

[5] Li L K, Yu Y J, Ye G J, Ge Q Q, Ou X D, Wu H, Feng D L, Chen X H and Zhang Y B 2014 *Nat. Nanotechnol.* **9** 372

[6] Castellanos-Gomez A, Vicarelli L, Prada E, Island J O, Narasimha-Acharya K L and Blanter S I 2014 *2D Materials* **1** 025001

[7] Xu M S, Liang T, Shi M M and Chen H Z 2013 *Chem. Rev.* **113** 3766

[8] Buscema M, Groenendijk D J, Blanter S I, Steele G A, Van d Z H S J and Castellanos-Gomez A 2014 *Nano Lett.* **14** 3347

[9] Li P K and Appelbaum I 2014 *Phys. Rev. B* **90** 115439

[10] Liu H, Neal A T, Zhu Z, Luo Z, Xu X F, Tománek D and Ye P D 2014 *ACS Nano* **8** 4033

[11] Tran V, Soklaski R, Liang Y and Yang L 2014 *Phys. Rev. B* **89** 235319

[12] Qiao J S, Kong X H, Hu Z X, Yang F and Ji W 2014 *Nat. Commun.* **5** 4475

[13] Fuhrer M S and Hone J 2013 *Nat. Nanotechnol.* **8** 146

[14] Xia F N, Wang, H and Jia Y C 2014 *Nat. Commun.* **5** 4458

[15] Koenig S P, Doganov R A, Schmidt H, Castro Neto A H and Özyilmaz B 2014 *Appl. Phys. Lett.* **104** 103106

[16] Deng Y X, Luo Z, Conrad N J, Liu H, Gong Y J, Najmaei S, Ajayan P M, Lou J, Xu X F and Ye P D 2014 *ACS Nano* **8** 8292

[17] Island J O, Steele G A, van der Zant H S and Castellanos-Gomez A 2015 *2D Materials* **2** 011002

[18] Fei R, Faghaninia A, Soklaski R, Yan J A, Lo C and Yang L 2014 *Nano Lett.* **14** 6393

[19] Flores E, Ares J R, Castellanos-Gomez A, Barawi M, Ferrer I J and Sánchez C 2015 *Appl. Phys. Lett.* **106** 022102

[20] Guo H, Lu N, Dai J, Wu X and Zeng X C 2014 *J. Phys. Chem. C* **118** 14051

[21] Li W, Zhang G and Zhang Y W 2014 *J. Phys. Chem. C* **118** 22368

[22] Wagner P, Ewels C P, Adjizian J J, Magaud L, Pochet P, Roche S and Briddon P 2013 *J. Phys. Chem. C* **117** 26790

[23] Xu H K, Ouyang G 2020 *Chin. Phys. B* **29** 037302

[24] Peng X, Copple A and Wei Q 2014 *J. Appl. Phys.* **116** 144301

[25] Huang J H, Wang X F, Liu Y S and Zhou L P 2019 *Nanoscale Res. Lett.* **14** 145

[26] Sisakht, E T, Zare, M H and Fazileh F 2015 *Phys. Rev. B* **91** 085409

[27] Tran V and Yang L 2014 *Phys. Rev. B* **89** 245407

[28] Ezawa M 2014 *New J. Phys.* **16** 115004

[29] Zhu Z L, Li C, Yu W Y, Chang D H, Sun Q and Jia Y 2014 *Appl. Phys. Lett.* **105** 113105

[30] Ren Y, Cheng F, Zhang Z H and Zhou G 2018 *Sci. Rep.* **8** 2932

[31] Tang Y, Zhou W, Hu C, Pan J and Ouyang F 2019 *Phys. Chem. Chem. Phys.* **21** 18551

[32] Chen N, Wang Y, Mu Y, Fan Y and Li S D 2017 *Phys. Chem. Chem. Phys.* **19** 25441

[33] Perkins F K, Friedman A L, Cobas E, Campbell P M and Jernigan G G 2013 *Nano Lett.* **13** 668

[34] Ordejón Pablo, Artacho E and Soler José M 1996 *Phys. Rev. B* **53** 10441

[35] Daniel Sánchez-Portal, Pablo Ordejón, Artacho E and José M Soler 1997 *Int. J. Quantum Chem.* **65** 453

[36] José M Soler, Artacho E, Gale J D, Alberto García and Daniel Sánchez-Portal Physics 2002 *J. Phys.: Condens. Matter* **14** 2745

[37] Perdew J P, Burke K and Ernzerhof M 1998 *Phys. Rev. Lett.* **80** 891

[38] Perdew J P, Burke K and Ernzerhof M 1996 *Phys. Rev. Lett.* **77** 3865

[39] Jia Y H, Gong P, Li S L, Ma W D, Fang X Y, Yang Y Y and Cao M S 2020 *Phys. Lett. A* **384** 126106